

Quantum Annealing Boosts Prediction of Multimolecular Adsorption on Solid Surfaces Avoiding Combinatorial Explosion

Hiroshi Sampei,[#] Koki Saegusa,[#] Kenshin Chishima, Takuma Higo, Shu Tanaka, Yoshihiro Yayama, Makoto Nakamura, Koichi Kimura, and Yasushi Sekine*

Cite This: *JACS Au* 2023, 3, 991–996

Read Online

ACCESS |

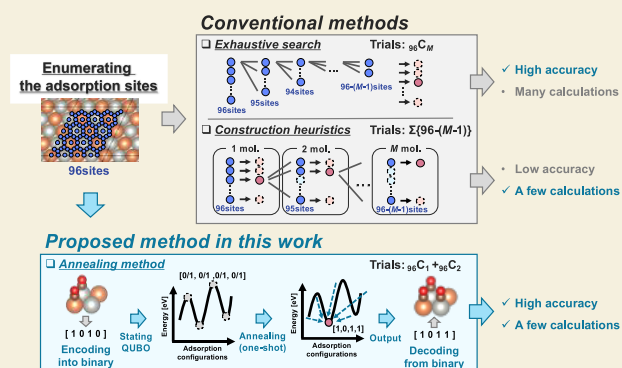
Metrics & More

Article Recommendations

Supporting Information

ABSTRACT: Quantum annealing has been used to predict molecular adsorption on solid surfaces. Evaluation of adsorption, which takes place in all solid surface reactions, is a crucially important subject for study in various fields. However, predicting the most stable coordination by theoretical calculations is challenging for multimolecular adsorption because there are numerous candidates. This report presents a novel method for quick adsorption coordination searches using the quantum annealing principle without combinatorial explosion. This method exhibited much faster search and more stable molecular arrangement findings than conventional methods did, particularly in a high coverage region. We were able to complete a configurational prediction of the adsorption of 16 molecules in 2286 s (including 2154 s for preparation, only required once), whereas previously it has taken 38 601 s. This approach accelerates the tuning of adsorption behavior, especially in composite materials and large-scale modeling, which possess more combinations of molecular configurations.

KEYWORDS: Quantum annealing, Multimolecular adsorption, Combinatorial explosion, Coverage



Quantum annealing has been used mostly in toy models (knapsack problem, traveling salesman problem) and logistics, but we were the first to successfully use it to predict molecular adsorption in chemistry. Molecular adsorption on solid surfaces is an important phenomenon of catalysis,¹ gas sensors,^{2,3} separation and purification processes,⁴ drug delivery,⁵ and surface modification.⁶ Fine control of adsorption behavior can therefore play an important role for energy conservation and sustainable societies. Adsorption properties are influenced not only by extrinsic factors such as temperature and pressure, but also by intrinsic factors of surface states such as the electronic state, steric structure, and coverage. Theoretical calculations are a powerful tool to ascertain both electronic and structural states and to simulate the adsorption phenomenon itself at the atomic level. However, because the number of candidate adsorption configurations corresponding to combinations of adsorption sites increases exponentially with the number of molecules, establishing a plausible molecular configuration for each coverage region by theoretical calculations has proven to be difficult. Such difficulty is attributed to combinatorial explosion.

To overcome this difficulty posed by the combinatorial explosion, quantum annealing (QA), an operation type of quantum computers, and QA-inspired methods have attracted attention.^{7,8} Actually, QA can solve combinatorial optimization problems known as quadratic unconstrained binary optimiza-

tion (QUBO) much faster and more accurately than classical computers because, in principle, QA can evaluate all combinations simultaneously using the quantum tunnelling effect and the quantum superposition.^{7,9} It has been used in problems related to biology,¹⁰ machine learning,¹¹ and materials science.¹² Also, information and communication technology¹³ have been applied to optimize the combinations. This feature has inspired us to use this method to elucidate surface states with adsorption.

As described herein, a QA-based method is reported for the first time to obtain plausible adsorption coordination within a realistic time range and irrespective of the number of adsorbed molecules (see Figure 1). Because the elucidation of its adsorption properties is useful in a wide variety of fields, this study was conducted with CO molecules adsorbed onto PdZn (111) surfaces, which were chosen because PdZn is an intermetallic compound, a solid surface with less symmetry than the pure metals used in many earlier adsorption studies,^{14,15} and CO is a promising chemical feedstock that

Received: January 9, 2023

Revised: March 11, 2023

Accepted: March 17, 2023

Published: March 27, 2023



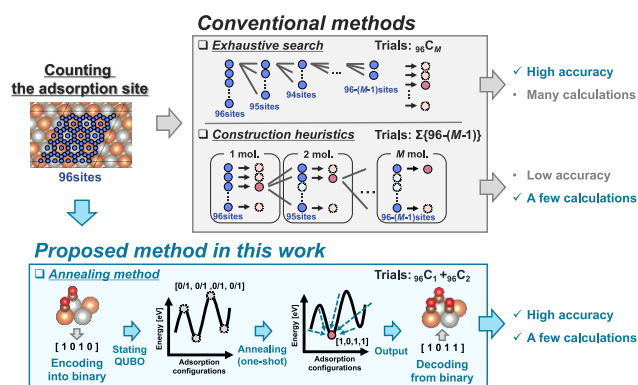


Figure 1. Schematic illustration of the searching method on the multimolecular adsorption configurations.

requires separation, detection, and reaction.^{3,16} PdZn alloys are also known as catalysts for CO-based methanol synthesis and various other reactions.¹⁷ Because this method requires only the results of theoretical calculations for unimolecular and bimolecular adsorption, the adsorption coordination can be predicted with far fewer trials (up to about 10^{14} times) than those used for conventional searches. Surprisingly, the adsorption energies can also be predicted accurately. Furthermore, the method can find more stable adsorption configurations, which are undiscoverable with feasible conventional methods. These results demonstrate that the annealing method can break through the trade-off in conventional searches between search costs and solution accuracy.

Initially, the QUBO problem was interpreted in the context of molecular adsorption on a surface. The objective function of QUBO with N variables is given as

$$\mathcal{H} = \sum_{i,j=1}^N W_{ij} \sigma_i \sigma_j + c \quad (1)$$

where W , σ_i , and c , respectively, represent the coefficient matrix (QUBO matrix) with a $W_{ij} = W_{ji}$ binary variable, and a constant value. Hereinafter, σ_i stands for 0 or 1, respectively, signifying conditions without or with adsorption on the i th adsorption site. In this situation, because $\sigma_i^2 = \sigma_i$, eq 1 is divisible into a term of diagonal components and a term of nondiagonal components as

$$\mathcal{H} = \sum_{i=1}^N \sum_{j>i}^N 2W_{ij} \sigma_i \sigma_j + \sum_{i=1}^N W_{ii} \sigma_i + c \quad (2)$$

Nondiagonal components are considered only in the upper triangular part because the QUBO matrix is symmetric. The annealing process finds $\sigma = [\sigma_1, \sigma_2, \dots, \sigma_N]$ to minimize \mathcal{H} . Definitions σ and \mathcal{H} as adsorption sites and adsorption energy are enabled to explore the most stable molecular arrangement by annealing because the search for the most stable adsorption configuration is synonymous with the search for a molecular arrangement with the lowest adsorption energy. To represent \mathcal{H} as the adsorption energy, suitable QUBO matrix construction is required. Here, the constant value c was set as 0 because the adsorption energy is 0 when adsorption does not occur anywhere (i.e., both σ_i and σ_j are 0). Because the second term in eq 2 is the first degree of σ_i , it denotes the sum of the contributions of each adsorption site to the adsorption energy. Considering unimolecular adsorption on the k th

adsorption site, the first term in eq 2 becomes 0 because at least either σ_i or σ_j is 0, and eq 2 is written as

$$\mathcal{H} = \sum_{i=1}^N W_{ii} \sigma_i = W_{kk} \sigma_k = W_{kk} \quad (3)$$

From eq 3, the diagonal components of the QUBO matrix can be set to unimolecular adsorption energies on each site. Additionally, the first term in eq 2 denotes the sum of the contributions of interaction between two adsorption sites to adsorption energy such as dipole–dipole interaction,¹⁵ because it is the second degree of σ_i . Considering bimolecular adsorption on the k th and l th adsorption sites, eq 2 is written as

$$\mathcal{H} = 2W_{kl} \sigma_k \sigma_l + W_{kk} \sigma_k + W_{ll} \sigma_l = 2W_{kl} + W_{kk} + W_{ll} \quad (4)$$

From eq 4 and from the discussion presented above, the nondiagonal components of the QUBO matrix can be set from the adsorption energies of single and double molecules. Based on these considerations, one can construct the QUBO matrix uniquely using the energies of these adsorptions because the numbers of adsorptions of one and two molecules are, respectively, equal to the numbers of the upper triangular parts of the diagonal and nondiagonal components of the matrix. Conversely, the QUBO matrix can derive the exact adsorption energies of unimolecular and bimolecular adsorption.

For this study, the adsorption/desorption behavior of CO molecules moving only perpendicularly to the PdZn (111) surface is investigated; Figure 2 presents a schematic

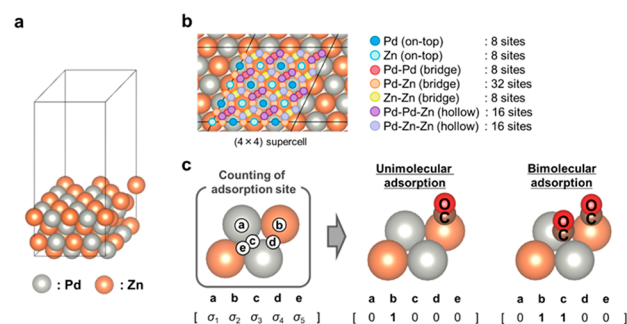


Figure 2. Surface configurations of PdZn alloy model. (a) Considered model of a PdZn surface. (b) Type and number of adsorption sites on PdZn surface. (c) Schematic image of the way to determine the binary variable matrix.

representation of the model considered in this study. Herein, N is 96 based on the results of the enumeration of adsorption sites. The adsorption energies for unimolecular and bimolecular adsorption were also calculated (Table S1 and Figure S1). These findings suggest that the bridge sites between Pd atoms are the most stable adsorption sites, even with increasing coverage. The calculated adsorption energies were used to construct a QUBO matrix satisfying eqs 3 and 4.

Then, the QUBO problem was solved under a constraint condition by annealing. First, annealing was performed using an equality constraint: the sum of σ_i is equal to the number of CO molecules M (Figures S2 and S3). Results indicated that CO adsorption leads to an energy increase in the system at the high-coverage region. Actually, molecular desorption takes place when adsorption is energetically unfavorable. Consequently, geometry optimization was conducted for the model

of 16 molecules adsorbed onto the predicted adsorption sites (Figure S4 and Table S2). The optimized structure indicated that, whereas molecules desorbed, they mutually interacted because of the high molecular density in the plane of the calculation cell. This constraint was unable to represent desorption properly. Therefore, a constraint considering desorption was researched. We assumed that the desorbed CO exists in the gas phase with no interaction. The adsorption energy, with m molecule adsorption and $M-m$ molecule desorption, is defined as

$$E_{\text{ad}} = (M-m) \times E(\text{CO}) + E(m\text{CO}/\text{PdZn}) - \{M \times E(\text{CO}) + E(\text{PdZn})\} \quad (5)$$

This eq 5 is just the eq 7 in the Supporting Information (Experimental Section) with m molecule adsorption itself. Therefore, the M molecule adsorption energy with some desorption is regarded as the adsorption energy with M or less molecular adsorption. The constraint is given as

$$\sum_{i=1}^N \sigma_i \leq M \quad (6)$$

The left side of eq 6 (i.e., the sum of σ_i) is 0 and more because σ_i is at least 0. Therefore, the lower limit of the sum of σ_i is not specified.

Second, annealing was performed using the inequality constraint. The results of annealing were compared with results obtained using other methods, construction heuristics, and inductive results from unimolecular and bimolecular adsorption. The procedures of all methods are shown in Figure S5 and the Experimental Section in the Supporting Information. No exhaustive search was conducted because there are 142 880 candidate combinations, even with trimolecular adsorption (${}_{96}C_3$, see Figure 5 to confirm the number of candidates for other multimolecular adsorption), and it needs enormous computational costs. The molecular arrangements obtained by annealing are depicted in Figures 3A

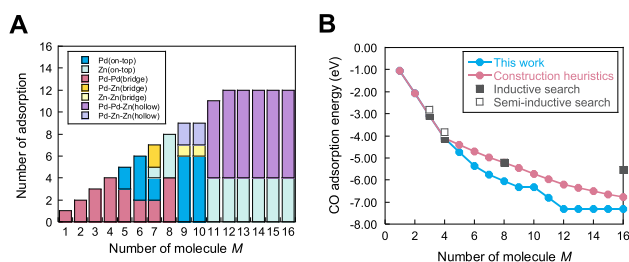


Figure 3. Predicted configurations of CO adsorption on PdZn surface with considering the desorption. (A) Predicted adsorption site for each number of CO molecule. (B) CO adsorption energy of adsorption configurations predicted by each method.

and S6. This result indicates that CO configurations drastically convert depending on the coverage. Moreover, desorption behaviors were observed in the high-coverage region. Additionally, the annealing results were compared with those obtained using other search methods (Figure 3B). Three and four molecules adsorption configurations in the inductive results were the same as those in the construction heuristic, hence the models of all CO adsorbed onto the on-top sites of Pd atom were also calculated as “semi-inductive results”. The molecular arrangements of the other methods are presented in

Figures S7 and S8. All energies were calculated after geometric optimization of the PdZn surface model located CO on the predicted adsorption sites. The annealing explored combinations of adsorption sites, most of which are no consideration in the other methods. The energies of the combination were equal to or more stable than those via the other methods because, in principle, annealing can search for all combinations, including those unexplored by other methods.^{7,9} This result implies that no more stable adsorption configurations can be found without searching for all combinations. It is noteworthy that desorption occurred in the construction heuristics when the number of CO was greater than 9 (Figure S9); adsorption energies appear to decrease despite desorbing because desorbed CO molecules form multilayer adsorption (Figure S10).

Finally, the adsorption energies of the theoretically calculated value and the predicted value from annealing were compared because the adsorption energies can be predicted from eq 1 using found σ . Figure 4 presents a comparison of

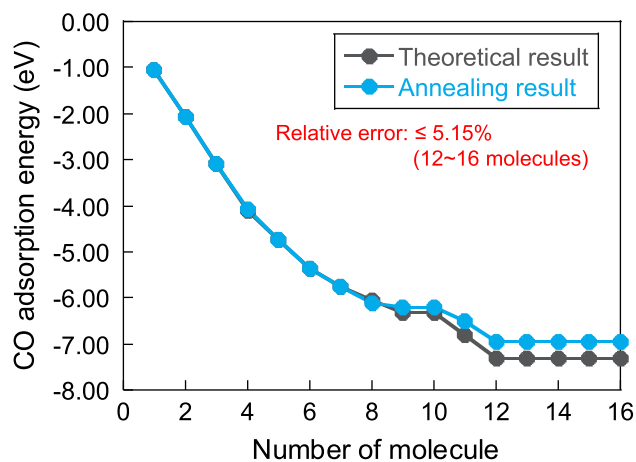


Figure 4. CO adsorption energy on the predicted adsorption configurations using the QUBO matrix and theoretical calculations.

theoretical calculations and the QUBO formula (eq 1) in adsorption energies for found σ . The values predicted using the QUBO matrix were close to the calculated values. This result indicates that the effect from the positional relation of adsorbates on adsorption energies is governed mainly by the one-molecule adsorption strength on each adsorption site and interactions between the two adsorbed molecules.

The numbers of calculations and the necessary time were measured to study the benefits of this annealing method in terms of predicting costs. Theoretical calculations were the most time-consuming process among these methods (Figure S5). Figure 5 depicts a comparison of the number of calculations. Because the annealing method only required unimolecular and bimolecular adsorption, for trimolecular adsorption and above, this method was performed in the smallest trial number among these methods except for trimolecular of the construction heuristics and with a constant trial number irrespective of the number of adsorptions. However, exhaustive searches and construction heuristics under M molecular adsorption require, respectively, ${}_{96}C_M$ and $\sum_{m=1}^M 96 - (m - 1)$ iterations of calculations. Therefore, the numbers of calculations for exhaustive searches increased exponentially as the combinatorial explosion and that for construction heuristics increased almost linearly. Figure 6

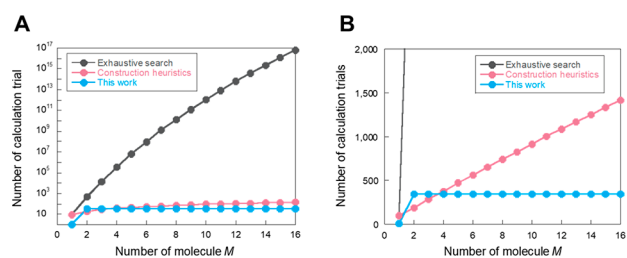


Figure 5. Calculation trial times on various search methods. The number of calculation trial with log scale (A) and with linear scale (B). The number of calculation trials in this work takes symmetry into account because it can determine symmetry in a realistic time by enumeration for unimolecular and bimolecular adsorption.

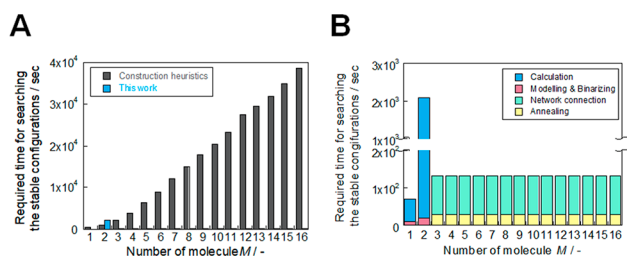


Figure 6. Consumed time for searching the most stable configurations. (A) Comparison between various search methods. (B) Classification of consumed times in annealing method.

depicts a comparison of the necessary time (detailed data available in Table S3). The time consumed for the annealing method was overwhelmingly favorable, especially in the high-coverage region (e.g., 16 molecule adsorption takes 132 s in this work, once the QUBO matrix was constructed, despite 38 601 s in the construction heuristics). In spite of the decreasing number of trials, the time consumed for construction heuristics was not saturated because of the trade-off between the computational cost of the increased atoms in the system and the number of empty adsorption sites. These results also indicate that the annealing method is superior in terms of predictive costs.

In summary, results of this study indicate that the search for the most stable adsorption configuration can be regarded as a kind of combinatorial optimization problem: QUBO. The adsorption configurations were predicted in feasible time ranges by solving QUBO, in principle searching for all combinations, because the proposed method requires only the information in unimolecular and bimolecular adsorption. The predicted molecular arrangements are more stable than the molecular configurations obtained via construction heuristics and inductive results from unimolecular and bimolecular adsorption, which implies that searching for all combinations is important to simulate adsorption behavior. Surprisingly, the adsorption energies predicted using the proposed method show good agreement with the value of theoretical calculations. Findings obtained from this study pave the way toward material designs for optimal adsorption properties in realistic coverage region, especially for large-scale modeling and composite materials such as high-entropy materials.

ASSOCIATED CONTENT

Supporting Information

The Supporting Information is available free of charge at <https://pubs.acs.org/doi/10.1021/jacsau.3c00018>.

Materials and methods, other supporting data (PDF)
CIF data and code files (ZIP)

AUTHOR INFORMATION

Corresponding Author

Yasushi Sekine – Department of Applied Chemistry, Waseda University, Tokyo 169-8555, Japan; orcid.org/0000-0001-6645-1961; Email: ysekine@waseda.jp

Authors

Hiroshi Sampei – Department of Applied Chemistry, Waseda University, Tokyo 169-8555, Japan; orcid.org/0000-0001-5844-2977

Koki Saegusa – Department of Applied Chemistry, Waseda University, Tokyo 169-8555, Japan

Kenshin Chishima – Department of Applied Chemistry, Waseda University, Tokyo 169-8555, Japan

Takuma Higo – Department of Applied Chemistry, Waseda University, Tokyo 169-8555, Japan

Shu Tanaka – Department of Applied Physics and Physico-Informatics, Keio University, Yokohama 223-8522, Japan; Green Computing System Research Organization, Waseda University, Tokyo 162-0042, Japan

Yoshihiro Yayama – Central Technical Research Laboratory, ENEOS Corporation, Yokohama, Kanagawa 100-8162, Japan

Makoto Nakamura – Quantum Research Center, Fujitsu Ltd., Kawasaki, Kanagawa 211-8588, Japan

Koichi Kimura – Quantum Research Center, Fujitsu Ltd., Kawasaki, Kanagawa 211-8588, Japan

Complete contact information is available at: <https://pubs.acs.org/10.1021/jacsau.3c00018>

Author Contributions

#H.S. and K.S. contributed equally. The manuscript was written through contributions of all authors. All authors have given approval to the final version of the manuscript.

Notes

The authors declare no competing financial interest.

ACKNOWLEDGMENTS

This work was partly achieved using the supercomputer system at the Information Initiative Center, Hokkaido University, Sapporo, Japan. Preferred Computational Chemistry provided the Matlantis for theoretical calculations. For annealing, DA3, Digital Annealer Ver.3 was provided by Fujitsu Ltd. This work was partially supported by Demonstration Project of Innovative Catalyst Technology for Decarbonization through Regional Resource Recycling, the Ministry of the Environment, Government of Japan.

REFERENCES

- (1) (a) Xie, C.; Yan, D.; Chen, W.; Zou, Y.; Chen, R.; Zang, S.; Wang, Y.; Yao, X.; Wang, S. Insight into the design of defect electrocatalysts: from electronic structure to adsorption energy. *Mater. Today* **2019**, *31*, 47–68. (b) Yang, Z. Z.; Wei, J. J.; Zeng, G. M.; Zhang, H. Q.; Tan, X. F.; Ma, C.; Li, X. C.; Li, Z. H.; Zhang, C. A

review on strategies to LDH-based materials to improve adsorption capacity and photoreduction efficiency for CO. *Coord. Chem. Rev.* **2019**, *386*, 154–182.

(2) (a) Li, Z.; Yao, Z.; Haidry, A. A.; Plecenik, T.; Xie, L.; Sun, L.; Fatima, Q. Resistive-type hydrogen gas sensor based on TiO₂: a review. *Int. J. Hydrog. Energy* **2018**, *43*, 21114–21132. (b) Kwak, D.; Lei, Y.; Maric, R. Ammonia gas sensors: a comprehensive review. *Talanta* **2019**, *204*, 713–730.

(3) Mahajan, S.; Jagtap, S. Metal-oxide semiconductors for carbon monoxide (CO) gas sensing: a review. *Appl. Mater. Today* **2020**, *18*, 100483.

(4) (a) Liang, C. Z.; Chung, T. S.; Lai, J. Y. A review of polymeric composite membranes for gas separation and energy production. *Prog. Polym. Sci.* **2019**, *97*, 101141. (b) Lin, R. B.; Xiang, S.; Zhou, W.; Chen, B. Microporous metal-organic framework materials for gas separation. *Chem.* **2020**, *6*, 337–363. (c) Bolisetty, S.; Peydayesh, M.; Mezzenga, R. *Chem. Soc. Rev.* **2019**, *48*, 463–487. (d) Azari, A.; Nabizadeh, R.; Nasser, S.; Mahvi, A. H.; Mesdaghinia, A. R. Comprehensive systematic review and meta-analysis of dyes adsorption by carbon-based adsorbent materials: classification and analysis of last decade studies. *Chemosphere* **2020**, *250*, 126238.

(5) (a) Mitchell, M. J.; Billingsley, M. M.; Haley, R. M.; Wechsler, M. E.; Peppas, N. A.; Langer, R. Engineering precision nanoparticles for drug delivery. *Nat. Rev. Drug Discovery* **2021**, *20*, 101–124. (b) Kotzabasaki, M.; Froudakis, G. E. Review of computer simulations on anti-cancer drug delivery in MOFs. *Inorg., Chem., Front.* **2018**, *5*, 1255–1272.

(6) (a) Lee, H.; Yoon, D. E.; Koh, S.; Kang, M. S.; Lim, J.; Lee, D. C. Ligands as a universal molecular toolkit in synthesis and assembly of semiconductor nanocrystals. *Chem. Sci.* **2020**, *11*, 2318–2329. (b) Geißler, D.; Budau, N. N.; Scholtz, L.; Tavernaro, I.; Genger, U. R. Analyzing the surface of functional nanomaterials – how to quantify the total and derivatizable number of functional groups and ligands. *Microchimica Acta* **2021**, *188*, 321. (c) Zhu, Q.; Murphy, C. J.; Baker, L. R. Opportunities for electrocatalytic CO₂ reduction enabled by surface ligands. *J. Am. Soc. Chem.* **2022**, *144*, 2829–2840.

(7) Kadowaki, T.; Nishimori, H. Quantum annealing in the transverse Ising model. *Phys. Rev. E* **1998**, *58*, 5355–5363.

(8) (a) Boixo, S.; Albash, T.; Spedalieri, F. M.; Chancellor, N.; Lidar, D. A. Experimental signature of programmable quantum annealing. *Nat. Commun.* **2013**, *4*, 2067. (b) Boixo, S.; Rønnow, T. F.; Isakov, S. V.; Wang, Z.; Wecker, D.; Lidar, D. A.; Martinis, J. M.; Troyer, M. Evidence for quantum annealing with more than one hundred qubits. *Nat. Phys.* **2014**, *10*, 218–224. (c) Rønnow, T. F.; Wang, Z.; Job, J.; Boixo, S.; Isakov, S. V.; Wecker, D.; Martinis, J. M.; Lidar, D. A.; Troyer, M. Defining and detecting quantum speedup. *Science* **2014**, *345*, 420–424. (d) Albash, T.; Vinci, W.; Mishra, A.; Warburton, P. A.; Lidar, D. A. Consistency tests of classical and quantum models for a quantum annealer. *Phys. Rev. A* **2015**, *91*, 042314. (e) Denchev, V. S.; Boixo, S.; Isakov, S. V.; Ding, N.; Babbush, R.; Smelyanskiy, V.; Martinis, J.; Neven, H. What is the computational value of finite-range tunneling? *Phys. Rev.* **2016**, *6*, 031015. (f) Mandrà, S.; Zhu, Z.; Wang, W.; Ortiz, A. P.; Katzgraber, H. G. Strengths and weaknesses of weak-strong cluster problems: a detailed overview of state-of-the-art classical heuristics versus quantum approaches. *Phys. Rev. A* **2016**, *94*, 022337. (g) Hauke, P.; Katzgraber, H. G.; Lechner, W.; Nishimori, H.; Oliver, W. D. Perspectives of quantum annealing: methods and implementations. *Rep. Prog. Phys.* **2020**, *83*, 054401. (h) Farhi, E.; Goldstone, J.; Gutmann, S.; Lapan, J.; Lundgren, A.; Preda, D. A. *Science* **2001**, *292*, 472. (i) Tanaka, S.; Tamura, R.; Chakrabarti, B. K. *Annealing and Computation*; Cambridge University Press, 2017.

(9) Lechner, W.; Hauke, P.; Zoller, P. A quantum annealing architecture with all-to-all connectivity from local interactions. *Sci. Adv.* **2015**, *1*, No. e1500838.

(10) (a) Perdomo-Ortiz, A.; Dickson, N.; Drew-Brook, M.; Rose, G.; Aspuru-Guzik, A. Finding low-energy conformations of lattice protein models by quantum annealing. *Sci. Rep.* **2012**, *2*, 571. (b) Li, R. Y.; Di Felice, R.; Rohs, R.; Lidar, D. A. Quantum annealing versus classical

machine learning applied to a simplified computational biology problem. *npj Quantum Inf.* **2018**, *4*, 14.

(11) (a) Adachi, S. H.; Henderson, M. P. Application of quantum annealing to training of deep neural networks. *arXiv (Quantum Physics)*, October 21, 2015, ver. 1, 1510.06356. (b) Benedetti, M.; Gómez, J. R.; Biswas, R.; Ortiz, A. P. Estimation of effective temperatures in quantum annealers for sampling applications: a case study with possible applications in deep learning. *Phys. Rev. A* **2016**, *94*, 022308. (c) Mott, A.; Job, J.; Vlimant, J. R.; Lidar, D.; Spiropulu, M. Solving a Higgs optimization problem with quantum annealing for machine learning. *Nature* **2017**, *550*, 375–379. (d) O'Malley, D.; Vesselinov, V. V.; Alexandrov, B. S.; Alexandrov, L. B. Nonnegative/binary matrix factorization with a D-Wave quantum annealer. *PLoS One* **2018**, *13*, No. e0206653.

(12) (a) Kitai, K.; Guo, J.; Ju, S.; Tanaka, S.; Tsuda, K.; Shiomu, J.; Tamura, R. Designing metamaterials with quantum annealing and factorization machines. *Phys. Rev. Res.* **2020**, *2*, 013319. (b) Hatakeyama-Sato, K.; Kashikawa, T.; Kimura, K.; Oyaizu, K. Tackling the challenge of a huge materials science search space with quantum-inspired annealing. *Adv. Intell. Syst.* **2021**, *3*, 2000209. (c) Imanaka, Y.; Anazawa, T.; Kumasaka, F.; Jippo, H. Optimization of the composition in a composite material for microelectronics application using the Ising model. *Sci. Rep.* **2021**, *11*, 3057. (d) Hatakeyama-Sato, K.; Adachi, H.; Umeki, M.; Kashikawa, T.; Kimura, K.; Oyaizu, K. Automated design of Li⁺-conducting polymer by quantum-inspired annealing. *Macromol. Rapid Commun.* **2022**, *43*, 2200385.

(13) (a) Neukart, F.; Compostella, G.; Seidel, C.; von Dollen, D.; Yarkoni, S.; Parney, B. Traffic flow optimization using a quantum annealer. *Front. ICT* **2017**, *4*, 29. (b) Ohzeki, M.; Miki, A.; Miyama, M. J.; Terabe, M. Control of automated guided vehicles without collision by quantum annealer and digital devices. *Front. Comput. Sci.* **2019**, *1*, 9. (c) Tanahashi, K.; Takayanagi, S.; Motohashi, T.; Tanaka, S. *J. Phys. Soc. Jpn.* **2019**, *88*, 061010.

(14) (a) Brix, F.; Desbuis, V.; Piccolo, L.; Gaudry, E. Tuning adsorption energies and reaction pathways by alloying: PdZn versus Pd for CO₂ hydrogenation to methanol. *J. Phys. Chem. Lett.* **2020**, *11*, 7672–7678. (b) Huang, Z. Q.; Long, B.; Chang, C. R. A theoretical study on the catalytic role of water in methanol steam reforming on PdZn (111). *Catal. Sci. Technol.* **2015**, *5*, 2935–2944. (c) Jeroro, E.; Lebarbier, V.; Datye, A.; Wang, Y.; Vohs, J. M. Interaction of CO with surface PdZn alloys. *Surf. Sci.* **2007**, *601*, 5546–5554. (d) Weilach, C.; Kozlov, S. M.; Holzappel, H. H.; Föttinger, K.; Neyman, K. M.; Rupprechter, G. Geometric arrangement of components in bimetallic PdZn/Pd(111) surfaces modified by CO adsorption: a combined study by density functional calculations, polarization-modulated infrared reflection absorption spectroscopy, and temperature-programmed desorption. *J. Phys. Chem. C* **2012**, *116*, 18768–18778.

(15) Föttinger, K. The effect of CO on intermetallic PdZn/ZnO and Pd₂Ga/Ga₂O₃ methanol steam reforming catalysts: a comparative study. *Catal. Today* **2013**, *208*, 106–112.

(16) Chauhan, D. K.; Sharma, N.; Kailasam, K. A critical review on emerging photocatalysts for syngas generation via CO₂ reduction under aqueous media: a sustainable paradigm. *Mater. Adv.* **2022**, *3*, 5274–5298.

(17) (a) Dang, S.; Yang, H.; Gao, P.; Wang, H.; Li, X.; Wei, W.; Sun, Y. A review of research progress on heterogeneous catalysts for methanol synthesis from carbon dioxide hydrogenation. *Catal. Today* **2019**, *330*, 61–75. (b) Ojelade, O. A.; Zaman, S. F. A review on Pd based catalysts for CO₂ hydrogenation to methanol: in-depth activity and DRIFTS mechanistic study. *Catal. Surv. Asia* **2020**, *24*, 11–37. (c) Liu, L.; Lin, Z.; Lin, S.; Chen, Y.; Zhang, L.; Chen, S.; Zhang, X.; Lin, J.; Zhang, Z.; Wan, S.; Wang, Y. Conversion of syngas to methanol and DME on highly selective Pd/ZnAl₂O₄ catalyst. *J. Energy Chem.* **2021**, *58*, 564–572. (d) Zhou, H.; Yang, X.; Li, L.; Liu, X.; Huang, Y.; Pan, X.; Wang, A.; Li, J.; Zhang, T. PdZn intermetallic nanostructure with Pd–Zn–Pd ensembles for highly active and chemoselective semi-hydrogenation of acetylene. *ACS Catal.* **2016**, *6*, 1054–1061. (e) Ma, M.; Han, X.; Li, H.; Zhang, X.; Zheng, Z.; Zhou, L.; Zheng, J.; Xie, Z.; Kuang, Q.; Zheng, L. Tuning electronic

structure of PdZn nanocatalyst via acid-etching strategy for highly selective and stable electrolytic nitrogen fixation under ambient conditions. *Appl. Catal., B* **2020**, *265*, 118568. (f) Furukawa, S.; Suzuki, R.; Komatsu, T. Selective activation of alcohols in the presence of reactive amines over intermetallic PdZn: efficient catalysis for alcohol-based N-alkylation of various amines. *ACS Catal.* **2016**, *6*, 5946–5953. (g) Wang, Y.; Wu, D.; Liu, T.; Liu, G.; Hong, X. Fabrication of PdZn alloy catalysts supported on ZnFe composite oxide for CO₂ hydrogenation to methanol. *J. Colloid Interface Sci.* **2021**, *597*, 260–268. (h) Torimoto, M.; Ogo, S.; Harjowinoto, D.; Higo, T.; Seo, J. G.; Furukawa, S.; Sekine, Y. Enhanced methane activation on diluted metal–metal ensembles under an electric field: breakthrough in alloy catalysis. *Chem. Commun.* **2019**, *55*, 6693–6695.